Calculation of ^{29}Si and ^{27}Al MAS NMR Chemical Shifts in Zeolite-β Using Density Functional Theory: Correlation with Lattice Structure

G. Valerio,[†] A. Goursot,*[,†] R. Vetrivel,[‡] O. Malkina,[§] V. Malkin,[⊥] and D. R. Salahub[||]

Contribution from Ecole Nationale Superiere de Chimie, Université de Montpellier, UMR 5618 CNRS, 8 rue de l'Ecole Normale, 34296 Montpellier Cédex 5, France, the Catalysis Division, National Chemical Laboratory, Pune 411008, India, the Computing Center, Slovak Academy of Sciences, Dubravska cesta 9, 84235 Bratislava, Slovak Republic, the Institute of Inorganic Chemistry, Slovak Academy of Sciences, Dubravska cesta 9, 84235 Bratislava, Slovak Republic, and the Département de Chimie, Université de Montréal, CP 6128, Montréal, Québec H3C3J7, Canada

Received March 17, 1998. Revised Manuscript Received July 28, 1998

Abstract: ^{29}Si and ^{27}Al NMR chemical shifts have been evaluated from the NMR shielding tensors obtained using the SOS-DFPT technique. The ^{29}Si NMR chemical shifts have been calculated for the nine crystallographically distinct Si sites of the zeolite-β lattice. The calculations were carried out on cluster models $Si(OSiH_3)_4$ and $R_3SiOSiR_3$ ($R = OSiH_3$) representing one (1T) and two (2T) sites in the zeolite lattice, respectively. Using the 1T models, the nine signals of the experimental spectrum have been assigned with a relative error of less than 1 ppm, the absolute error being estimated at about 5 ppm. The use of a "fragment-averaging" technique based on the results obtained with the 2T models leads to calculated absolute NMR shifts with an accuracy of ±1 ppm. The ^{27}Al NMR shifts of $AlH(OSiH_3)_4$ models have also been calculated, after relaxation of the local geometry. It was found that the relative positions of the ^{27}Al chemical shifts are in agreement with the experimental spectrum.

I. Introduction

The zeolite-β is one of the first few high-silica zeolites to be prepared using organic additives.[1] Its framework structure is complex, due to stacking disorder and also to highly intergrown hybrids of two distinct structures, namely, polymorphs A and B.[2−4] The aluminosilicate β zeolite has been synthesized with varying Si/Al ratio.[5−8] It is a large-pore zeolite, which exhibits a strong Brønsted acidity, typical of high-silica zeolites, and this acidity is fine-tuned by the incorporation of several other trivalent elements, such as boron, vanadium, chromium, lanthanum, gallium, titanium, iron, etc. in the framework.[9]

Catalytically, zeolite-β has been utilized for several acid-catalyzed reactions,[10] such as cracking, hydrocracking, dewaxing, alkylation/dealkylation, alkoxylation, and deNOx. The acidity in zeolite-β has been characterized and its acidic properties have been modified by altering the synthesis procedures, to improve its catalytic properties.[11]

NMR spectroscopy has been extensively used to study various characteristics of zeolite-β, for example, the internal void space,[12] the crystallographically distinct Si sites,[13] dealumination processes,[14] and the coordination state of aluminum.[15] Indeed, the recent development of high-resolution solid-state NMR, such as magic-angle spinning (MAS), has induced extensive studies of the composition and structure of zeolite frameworks[16] as well as in situ reactions.[17] This high resolution allows the detection of small structural differences as those induced by temperature variations or by crystallographically inequivalent environments of silicon sites. The traditional assignment of ^{29}Si NMR spectra of zeolites is essentially based on empirical relations derived from the dependence on geometry of the observed chemical shifts.[18−20] Moreover, the analysis of deshielding effects due to the presence of Al tetrahedra has led to linear relationships

* To whom correspondence should be addressed.
[†] Université de Montpellier.
[‡] National Chemical Laboratory.
[§] Computing Center, Slovak Academy of Sciences.
[⊥] Institute of Inorganic Chemistry, Slovak Academy of Sciences.
[||] Université de Montréal.

(1) Wadlinger, R. L.; Kerr, G. T.; Rosinski, E. J. U.S. Patent No. 3308069 (assigned to Mobil Oil Corporation), 1967.
(2) Newsam, J. M.; Treacy, M. M. J.; Koetsier, W. T.; De Gruyter, C. B. *Proc. R. Soc. London, A* **1988**, *420*, 375.
(3) Treacy, M. M.; Newsam, J. M. *Nature* **1988**, *332*, 249.
(4) Higgins, J. B.; La Pierre, R. B.; Schlenker, J. L.; Rohrman, A. C.; Wood, J. D.; Kerr, G. T.; Rohrbaugh, W. J. *Zeolites* **1988**, *8*, 446.
(5) Bond, A. E.; Burgess, C. G. V.; Martin, D. E. U.S. Patent No. 3793385 (assigned to BPPLC (U.K.)), 1974.
(6) Robson, H. E. U.S. Patent No. 4560542 (assigned to Exxon Research and Engineering Company), 1985.
(7) Rubin, M. K. Eur. Pat. Appl. EP 159846 (assigned to Mobil Oil Corporation), 1985.
(8) Perez-Pariente, J.; Martens, J. A.; Jacobs, P. A. *Zeolites* **1988**, *8*, 46.
(9) Camblor, M. A.; Corma, A.; Perez-Pariente, J. *Zeolites* **1993**, *13*, 82.
(10) Bellusi, G.; Pazzuconi, G.; Perego, C.; Girotti, G.; Terzoni, G. *J. Catal.* **1995**, *157*, 227.
(11) Caullet, P.; Hazm, J.; Guth, J. L.; Joly, J. F.; Lynch, J.; Raatz, F. *Zeolites* **1992**, *12*, 240.
(12) Benslama, R., Fraissard, J.; Albizane, A.; Fajula, F.; Figueras, F. *Zeolites* **1988**, *8*, 196.
(13) Fyfe, C. A.; Strobl, H.; Kokotailo, G. T.; Pasztor, C. T.; Barlow, G. E.; Bradley, S. *Zeolites* **1988**, *8*, 132.
(14) Perez-Pariente, J.; Sanz, J.; Fornes, V.; Corma, A. *J. Catal.* **1990**, *124*, 217.
(15) Bourgeat-Lami, E.; Massiani, P.; Di Renzo, F.; Espiau, P.; Fajula, F. *Appl. Catal.* **1991**, *72*, 139.
(16) Fyfe, C. A.; O'Brien J. H.; Strobl, H. *Nature* **1987**, *326*, 281.
(17) *NMR Techniques in Catalysis*; Bell, A. T., Pine, A., Eds.; Marcel Dekker: New York, 1994.
(18) Newsam, J. M. *J. Phys. Chem.* **1987**, *91*, 1259.
(19) Radeglia, R,; Engelhardt, G. *Chem. Phys. Lett.* **1985**, *114*, 28.
(20) Fyfe, C. A.; Grondey, H.; Feng, Y.; Kokotailo, G. T. *J. Am. Chem. Soc.* **1990**, *112*, 8812.

10.1021/ja980903g CCC: $15.00
Published on Web 10/27/1998

between the ^{29}Si chemical shifts and the number of Al neighbors.[21] These empirical predictions have been shown to be useful in determining the distribution of aluminum in faujasite lattice.[22]

The ab initio theoretical prediction of NMR properties started with the early work by Ditchfield,[23] who proposed the GIAO method, later implemented in nonempirical Hartree−Fock calculations[24,25] and post Hartree−Fock[26] calculations. Although this method has been applied to predict the chemical shifts of organic compounds, its application to zeolite structures has still been limited to a few applications. Using this method, ^{1}H and ^{29}Si chemical shifts have been calculated for model clusters of symmetrical silicate species.[27] Very recently, the coupled perturbed Hartree−Fock method has been used to predict ^{29}Si NMR spectra of α-quartz and several zeolitic structures[28] and to interpret the ^{17}O NMR spectrum of a siliceous faujasite.[29] There were few attempts[30−32] at modeling NMR shielding constants within the framework of density functional theory (DFT), restricted to uncoupled DFT response theory. Very recently, the sum-over-states density functional perturbation theory (SOS-DFPT) approach has been proposed[33] and demonstrated to be a very efficient and accurate procedure to calculate NMR shielding tensors.[33−35]

Success in simulating the NMR properties of fully siliceous and aluminosilicate zeolite frameworks would have far-reaching consequences: (i) the assignment of the different MAS NMR signals to crystallographically distinct Si or Al sites; (ii) the correlation between observed NMR spectral changes and structural modifications of the zeolite framework; (iii) the easier prediction of in situ reaction mechanisms. The aim of this work is thus to verify if, using the SOS-DFPT methodology, the description and assignment of the complex ^{29}Si and ^{27}Al NMR spectra of zeolite-β can be performed with sufficient accuracy. For more clarity, the study of the choice of the basis set and of the exchange and correlation functionals has been performed on a simpler zeolite with only two crystallographic sites, i.e., the zeolite mazzite. These results as well as a detailed analysis of the geometrical and electronic factors on the calculated chemical shifts are reported elsewhere.[36] However, we will incorporate in this paper the calculated ^{29}Si chemical shifts of mazzite for 1T and 2T models, to show that the same general trends concerning the effect of the cluster size are derived from both studies. Finally, we propose a simple procedure which allows an accuracy of about 1−2 ppm without requiring very large computational resources.

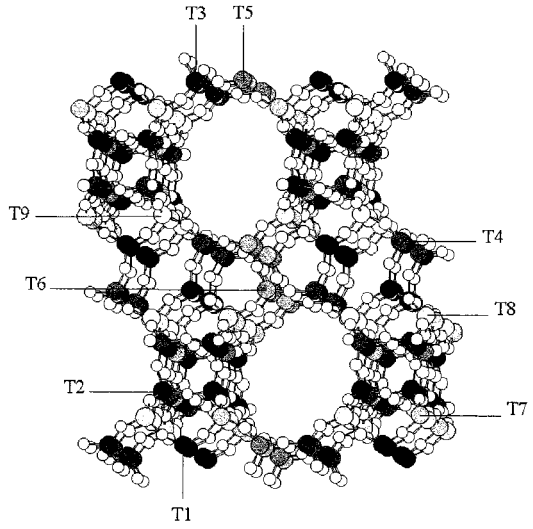

Figure 1. Framework structure of polymorph A of zeolite-β, viewed along the (010) axis, with the nine T sites (light gray, medium gray, and black colors correspond to sites of group B, C, and A, respectively).

II. Models

There are nine crystallographically distinct "T" sites in zeolite-β. We considered the experimental structure of polymorph A, reported by Newsam et al.[2] Due to the stacking disorder of this zeolite, the atomic coordinates used in this study may lead to some uncertainty when sites have very comparable local geometries and thus very similar chemical shifts. The framework structure of zeolite-β as viewed along the (010) axis showing the 12-membered ring pores and the distribution of the nine T sites is given in Figure 1. A table with the detailed description of the geometry and connectivity of the Si−O−Si linkages around the nine crystallographic sites is available as Supporting Information.

Two kinds of cluster models have been considered in this study. In Figure 2a a one-site (1T) cluster is shown, with formula $Si(OSiH_3)_4$. Nine different clusters of this kind (denoted as mSi) have been used to model the nine crystallographic sites of zeolite-β. The three types of two-site models (2T), hereafter denoted mSiOSi, which originate from the β structure are shown in Figure 2b−d. These clusters are of the type $R_3SixOSiyR_3$ ($R = OSiH_n$, $n = 3$) and have respectively zero, one, and two four-membered rings, following the local connectivity between the two sites.

In all the clusters that we have considered, the dangling bonds have been saturated with hydrogen atoms. The Si−H bond distance has been set to 1.50 Å, and the H atoms have been positioned along the corresponding Si−O bond vectors in the experimental structure.

Model clusters of the one-site type were also used to study the substitution of silicon by aluminum. In these models (denoted as mAlH), H^+ counterions are added to compensate the negative charge following the substitution. The preferred O sites for the initial counterion positions before optimization were defined as the molecular electrostatic potential (MEP) minima, following the results of a previous study.[37]

(21) Newsam, J. M. *J. Phys. Chem.* **1985**, *89*, 2002.
(22) Himei, H.; Yamadaya, M.; Oumi, Y.; Kubo, M.; Stirling, A.; Vetrivel, R.; Broclawik, E.; Miyamoto, A. *Microporous Mater*. **1996**, *7*, 235.
(23) Ditchfield, R. *Mol. Phys.* **1974**, *27*, 789.
(24) Ahlrichs, R.; Bar, M. M.; Haser, M.; Horn, H.; Kolmel, C. *Chem. Phys. Lett.* **1989**, *162*, 165.
(25) Haser, M.; Ahlrichs, R.; Baron, H. P.; Weis, P.; Horn, H. *Theor. Chim. Acta* **1992**, *83*, 455.
(26) Fleischer, U.; Kutzelnigg, W.; Bleiber, A.; Sauer, J. *J. Am. Chem. Soc.* **1993**, *115*, 7833.
(27) Moravetski, V.; Hill, J.; Eichler, U.; Cheetam, AK.; Sauer, J. *J. Am. Chem. Soc.* **1996**, *118*, 13015.
(28) Bussemer, B.; Scröder, K. P.; Sauer, J. *Solid State Nucl. Magn. Reson.* **1997**, *9*, 155.
(29) Bull, L. M.; Cheetham, A. K.; Anupold, T.; Reinhold: A.; Samoson, A.; Sauer, J.; Bussemer, B.; Lee, Y.; Gann, S.; Shore, J.; Pines, A.; Dupree, R. *J. Am. Chem. Soc.* **1998**, *120*, 3510.
(30) Bieger, W.; Seifert, G.; Eschrig, H.; Grossmann, G. *Chem. Phys. Lett.* **1986**, *115*, 275.
(31) Freier, D. A.; Fenske, R. F.; Xiao-Zeng, Y. *J. Chem. Phys.* **1985**, *83*, 3526.
(32) Friedrich, K.; Seifert, G.; Grossmann, G. *Z. Phys. D* **1990**, *17*, 45.
(33) Malkin, V. G.; Malkina, O. L.; Casida, M. E.; Salahub, D. R. *J. Am. Chem. Soc.* **1994**, *116*, 5898.
(34) Kaupp, M.; Malkin, V. G.; Malkina, O. L.; Salahub, D. R. *Chem. Phys. Lett.* **1995**, *235*, 382.
(35) Malkin, V. G.; Malkina, O. L.; Salahub, D. R. *J. Am. Chem. Soc.* **1995**, *117*, 3294.
(36) Valerio, G.; Goursot, A. To be published.
(37) Papai, I., Goursot, A.; Fajula, F.; Weber, J. *J. Phys. Chem.* **1994**, *98*, 4654.

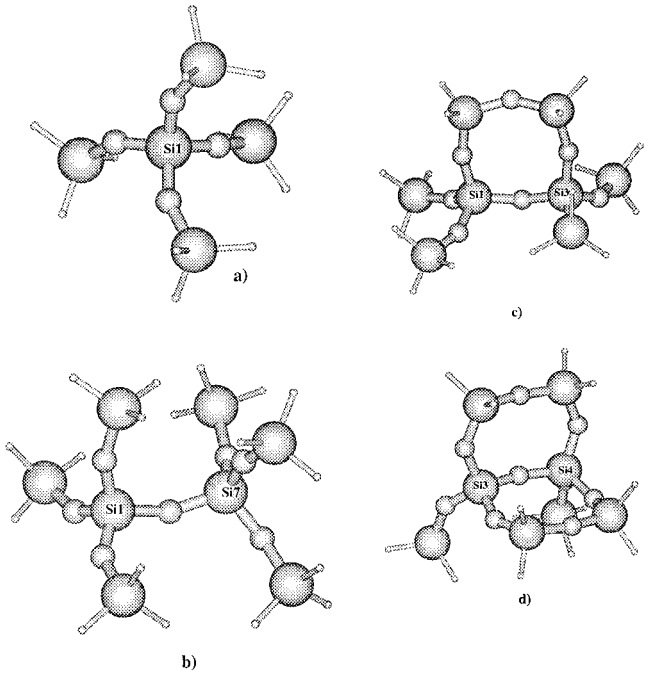

Figure 2. (a) Typical mSi cluster model representing the Si1 site in polymorph A of zeolite β. (b−d) Typical mSi*x*Si*y* cluster models. These cluster models represent zero, one, or two four-membered rings formed because of different connectivities of adjacent Si sites. Large circles are Si, medium circles O, and small circles H.

III. Methods

The calculations have been performed within the linear combination of Gaussian type orbitals−density functional formalism (LCGTO-DF),[38−40] using the deMon and deMon properties programs.[33,41,42]

The experimental geometry has been adopted for the highly siliceous models.[2] To take into account the relaxation of the structure when Si is replaced by Al, the terminal H atoms of the cluster models have been fixed and all the other atoms allowed to move, in a geometry optimization calculation.

The intent is to optimize the local geometry simulating, with the fixed boundaries, the rigid component given by the whole zeolitic lattice. The size of an Al ion is not so much different from that of Si (the Al−O bond distances in zeolites are about 0.1−0.2 Å longer than Si−O), and it has been argued that the relaxation following the Si → Al substitution is a purely local phenomenon,[43] so that even relatively small clusters can give reliable geometries.

All geometry optimizations have been performed at the gradient-corrected density functional level of Becke[44] functional for exchange and Perdew[45] for correlation.

For geometry optimization, all-electron basis sets of DZP quality have been used for all heavy atoms whereas the terminal hydrogens have been described by a smaller DZ basis. In Huzinaga's notation the contraction patterns are (6321/521/1), for Si and Al, (621/41/1) for O, and (41) for H.[46]

Table 1. Calculated ^{29}Si NMR Shielding Constants and Chemical Shifts (ppm) for 1T Models Compared with Experimental δ Values[13]

Si sites	⟨TOT⟩	σ, δ_{calc}	δ_{exp}
1	155.3	457.9, −113.0	−115.5
2	155.9	458.1, −113.2	−116.0
3	148.0	451.5, −106.6	−111.0
4	148.2	451.8, −106.9	−111.6
5	151.8	454.3, −109.4	−112.0
6	152.2	454.8, −109.9	−113.0
7	152.8	455.9, −111.0	−113.2
8	151.4	454.9, −110.0	−111.8
9	149.7	453.7, −108.8	−111.7

The associated auxiliary basis sets used to fit the density and the exchange-correlation potential are for the same atoms (5,4;5,4), (5,2;5,2), and (5,1;5,1), respectively, where the usual deMon notation is used.[37] A grid of 64 radial points has been used for the evaluation of the exchange-correlation potential and energies during the geometry optimizations. The single-point NMR calculations used a 32 radial grid for the V_{xc} fitting. As suggested by Malkin et al.,[33] more precise molecular orbital coefficients are obtained by performing an additional iteration after SCF convergence using the numerical evaluation of the exchange-correlation potential on an enlarged grid.

The NMR shielding tensors have been calculated with the sum-over-states density functional perturbation theory (SOS-DFPT) in the LOC1 approximation,[33] along with the IGLO method for the choice of the gauge origin.[47] The IGLO III basis set of Kutzelnigg et al.[47] was used for all the heavy atoms, keeping the standard (41) basis for the terminal H. Only the shielding tensors of the two central T atoms (T = Si, Al) were considered, because only these atoms have an appropriate local environment. All the shielding tensor calculations were performed using the PW91 functional.[48]

IV. Results and Discussion

1. One-Site Cluster Models. We first carried out calculations on the one-site (mSi) clusters representing each one of the nine crystallographic sites, as mentioned in an earlier section. A similar calculation was also performed for tetramethylsilane (TMS), and the chemical shifts (δ) reported for the various silicon sites are obtained using TMS as a reference. In Table 1, the calculated δ values are presented for the models representing the nine sites together with the experimental chemical shifts and average Si−O−Si angles. Although the average Si−O bond distance in the nine distinct SiO_4 units does not vary significantly (cf. Table 2 for sites 1, 3, and 8), the average Si−O−Si bond angles show a variation of 7.9° between the lowest value of 148.0° (Si3 site) and the highest value of 155.9° (Si2 site).

Fyfe et al.[13] have reported the ^{29}Si MAS NMR spectrum for a siliceous zeolite-β. Despite the stacking disorder in the solid, this high-resolution spectrum could be deconvoluted into nine distinct signals. This might indicate that the ^{29}Si NMR screening constant is a local property, allowing us to anticipate a reasonably good description even using small model clusters. There have been attempts in the literature to correlate NMR shifts to geometric parameters such as T−T distances[13,19] and T−O−T angles.[20] Moreover, the ^{29}Si chemical shifts are sensitive to neighboring aluminum atoms and hence to the T−T distance, being systematically shifted downfield by approximately 5−10 ppm for every additional Al atom in the first

(38) Sambe, H., Felton, R. H. *J. Chem. Phys.* **1975**, *62*, 1122.
(39) Dunlap, B. I.; Conolly, J. W. D.; Sabin, J. R. *J. Chem. Phys.* **1979**, *71*, 3396.
(40) Salahub, D. R. *Adv. Chem. Phys.* **1987**, *69*, 447.
(41) St-Amant, A.; Salahub, D. R. *Chem. Phys. Lett.* **1990**, *169*, 387.
(42) Casida, M. E.; Daul, C. D.; Goursot, A.; Koester, A.; Petterson, L.; Proynov, E.; St-Amant, A.; Salahub, D. R.; Duarte, H.; Godbout, N., Guan, J.; Jamorski, C.; Leboeuf, M.; Malkin, V.; Malkina, O.; Sim, F.; Vela, A.; deMon Software − deMon40KS3 Module, University of Montreal, 1996.
(43) Kramer, G. J.; de Man, A. J. M.; van Santen, R. A. *J. Am. Chem. Soc.* **1991**, *113*, (3), 6435.
(44) Becke, A. D. *Phys. Rev. A* **1988**, *38*, 3098.
(45) Perdew, J. P. *Phys. Rev. B* **1986**, *33*, 8822; erratum *Phys. Rev. B* **1986**, *34*, 7406.
(46) Godbout, N.; Salahub, D. R.; Andzelm, J.; Wimmer, E. *Can. J. Chem.* **1992**, *70*, 560.
(47) Kutzelnigg, W.; Fleischer, U.; Schindler, M. *NMR-basic principles and progress*; Springer-Verlag: Heidelberg, 1990; Vol. 23, p 165.
(48) Perdew, J. P.; Wang, Y. *Phys. Rev. B* **1992**, *45*, 13244. Perdew, J. P.; Chevary, J. A.; Vosko, S. H.; Jackson, K. A.; Pederson, M. R.; Singh, D. J.; Fiolhais, C. *Phys. Rev. B* **1992**, *46*, 6671.

Table 2. T−O Bond Distances (Å) and T−O−Si Bond Angles (deg) with T = Si or Al in the 1T Cluster Models after Geometry Optimization, Compared with the Experimental Values

	mSi (exp)	mSi (opt)	mAlH (opt)
	Site 1		
T1−O10	1.616	1.636	1.699
T1−O11	1.617	1.631	1.906
T1−O12	1.616	1.634	1.708
T1−O13	1.617	1.627	1.717
∠TO10Si2	163.2	157.6	162.8
∠TO11Si3	148.3	143.5	135.1
∠TO12Si7	156.4	150.9	135.3
∠TO13Si8	153.3	148.6	132.7
	Site 3		
T3−O11	1.614	1.641	1.714
T3−O30	1.616	1.637	1.714
T3−O31	1.615	1.636	1.724
T3−O32	1.616	1.629	1.889
∠TO11Si1	148.3	143.3	130.7
∠TO30Si4	162.3	159.9	148.0
∠TO31Si5	137.5	135.0	123.8
∠TO32Si8	143.9	137.8	130.2
	Site 8		
T8−O13	1.615	1.641	1.714
T8−O21	1.617	1.637	1.712
T8−O32	1.616	1.633	1.900
T8−O61	1.617	1.628	1.714
∠TO13Si1	153.3	149.7	137.6
∠TO21Si2	157.8	155.0	146.8
∠TO32Si3	143.9	138.2	130.8
∠TO61Si6	150.7	145.0	131.2

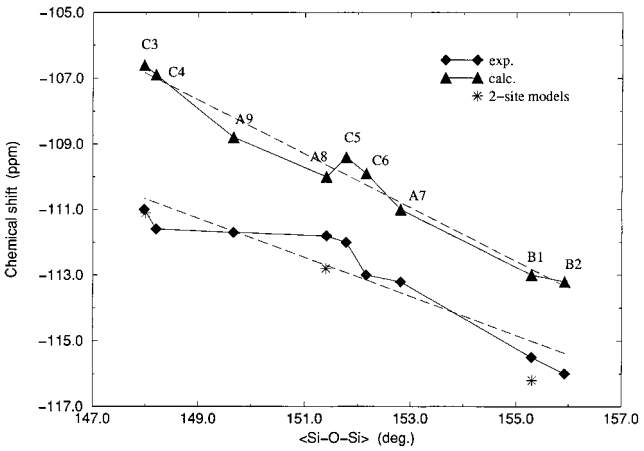

Figure 3. Variation of δ with ⟨SiOSi⟩ angles for 1T (triangles) and 2T clusters (stars) compared with experimental data (diamonds), taken from ref 13. The dashed straight lines represent the linear fit for both experimental and calculated δ.

tetrahedral coordination sphere of the silicon atom.[49] In contrast, for highly siliceous zeolites, the average Si−O−Si bond angle seems to have the best correlation with chemical shift values.[20] As shown from Table 1, the lowest δ value (highest σ) is assigned to the T site with the largest ⟨T−O−T⟩ angle.

Figure 3 shows the plot of both the experimental and calculated chemical shifts against the Si−O−Si bond angles. A qualitative linear correlation is observed in both cases with a few minor deviations. It is gratifying to observe the 1:1 correlation between the experimental and calculated chemical shifts of the various T sites. The same trend has also been obtained for mazzite: the calculated δ values (average ⟨Si−O−Si⟩ angles) are −109.2 ppm (152.5°) and −100.2 ppm (141.3°), for sites 1 and 2, respectively. These results also prove that the linear correlation assumed between the chemical shift and the average ⟨T−O−T⟩ bond angle is valid. They also prove that 1T models can be used to describe relative chemical shifts, the error being less than 2 ppm for zeolite-β and less than 1 ppm for mazzite. However, the size of these clusters is not sufficient to describe absolute δ values with a precision better than 1−5 ppm for zeolite-β and 3−4 ppm for mazzite (δ_{exp}(site 1) = −113.1; δ_{exp}(site 2) = −103.4 ppm). It is interesting to compare our results (1T and 2T models) with those obtained in the study of Bussemer et al.[28] They have calculated the ^{29}Si shifts of α-quartz and five siliceous zeolites with a CPHF-GIAO method using three shells of neighbors (O, Si, O) around the central silicon. These models are, in some sense, intermediate between our 1T and 2T models (with averaging technique). They obtain, at the experimental geometry, a low-field shift of approximately 4 ppm with respect to the experimental spectra, which is comparable with the shift obtained with our 1T models.

The study of the correlation between the electronic structure of the zeolite and the chemical shifts is not straightforward, expecially when neighboring silicons are replaced by other elements. Several proposals have been made in the literature to correlate ^{29}Si shifts and electronic properties of neighboring O and T atoms.[19,50,51] The analysis of the contributions of the various localized molecular orbitals to the screening tensors of the different ^{29}Si sites in zeolite-β shows that the variation of the paramagnetic term (negative) is dominant. The main paramagnetic contribution originates from the Si−O bonding orbitals and increases with decreasing ⟨T−O−T⟩ angles.

Topographically, the nine T sites in zeolite-β could be grouped into three categories, namely, A, B, and C as described earlier.[37] In group A, a given T site is not associated with any four-membered ring whereas in groups B and C, the T sites belong to one and two four-membered rings, respectively. T sites 7, 8, and 9 come under group A, 1 and 2 come under group B, and 3, 4, 5, and 6 come under group C. Although the experimental spectrum shows indeed three groups of signals, it can be observed from Figure 3 that, if upfield signals are exclusively due to group B sites, the two downfield signals are found to be arising from both groups A and C. Thus, the chemical shifts cannot be correlated to the topography of Si sites only.

A. Geometry Relaxation of Si-Containing Clusters. To verify the incidence of geometry optimization on our results, we have chosen three representative cluster models of groups B, C, and A, namely, T1, T3, and T8, and optimized their geometry, as described in Section III. Their calculated structures are compared with experimental values in Table 2, whereas the corresponding ^{29}Si chemical shifts are displayed in Table 3.

As seen from Table 2, the calculated Si−O bond lengths are regularly too long, by 0.01−0.03 Å, whereas the Si−O−Si bond angles are 4−5° too small. These differences with respect to the experimental geometry of the solid occur systematically for the three models and result from the limited size of the 1T clusters. As a consequence of the decreased value of the average Si−O−Si bond angle, the calculated δ values are also systematically decreased, following the above-mentioned correlation between smaller angles and less negative chemical shifts.

The calculated chemical shifts for the optimized models are

(49) Engelhardt, G.; Michel, D. *High-resolution solid-state NMR of silicates and zeolites*, John Wiley: New York, 1987.

(50) Ramdas, S.; Klinowski, J. *Nature (London)* **1984**, *308*, 521.

(51) Weller, M. T.; Dann, S. E.; Johnson, G. M.; Mead, P. J. In *Progress in Zeolites and Micoporous Materials*; Chon, H., Ihm, S. K., Uh, Y. S., Eds.; Studies in Surface Science and Catalysis; Elsevier Science B. V.: New York, 1997, Vol. 105, p 455.

Table 3. ^{29}Si and ^{27}Al NMR Shielding Constants and Chemical Shifts, ppm, Calculated for the 1T Cluster Models Representing Sites 1, 3, and 8 after Optimization and Compared with Experimental δ Values[13,14]

site	$\langle$TOT$\rangle_{opt}$	σ, δ_{calc}	δ_{exp}
Si1	150.2	453.1, −108.2	−115.5
Si3	144.0	446.8, −101.9	−111.0
Si8	147.0	449.4, −104.5	−111.8
Al1	141.5	501.5, −95.1	−106.0
Al3	133.2	495.3, −88.9	−99.5
Al8	136.6	497.8 −91.4	−103.0

then 7−9 ppm lower than the experimental values. We can thus estimate at around 5 ppm the error due to the cluster size effect on the geometry (leading to underestimated δ values) and at 2−4 ppm the error due to the cluster size effect on the modeling of δ itself. Of course, there are also systematic errors due to the methodology (SOS-DFPT, basis sets, etc.), but they should be partly canceled in the difference with the screening constant of the reference compound. Morever, the large shift provided by the use of 2T models (next subsection) shows that the cluster size is a major source of error when absolute δ values are considered.

Small 1T models are sufficient to describe relative chemical shifts among the different sites of a given zeolite, even if the error on the absolute δ values is increased by geometry optimization. This situation indeed occurs when Si sites are substituted by other elements. Larger clusters are necessary for a more precise description of the absolute chemical shifts (see further below).

B. Geometry Optimization of Al-Containing Clusters Models. ^{27}Al NMR shielding constants and chemical shifts have been calculated for representative sites of groups B, C, and A, namely, sites T1, T3, and T8. The calculation of σ was carried out for the trimethylaluminum (TMA), and the δ values reported for various Al sites are obtained using TMA as the reference. The experimental chemical shifts for ^{27}Al are usually determined with respect to $Al(NO_3)_3$ in aqueous solution. Modeling this species as $Al(H_2O)_6^{3+}$ (T_h symmetry) corresponds to an uncertainty of more than 10 ppm for its ^{27}Al shielding constant, leading us to the conclusion that this representation of the solvated reference complex is too simple.[36] The use of TMA (dimer) as the calculated reference and of the gas-phase experimental δ(TMA) value with respect to $Al(NO_3)_3$ in aqueous solution allows this difficulty to be avoided.

Since the experimental crystal structure is not available for zeolite Al-β, the geometry of the cluster models mAlH has been optimized. We can expect from our results on the mSi models and also from an earlier study[37] that the geometry optimization will lead to slightly overestimated Al−O bond lengths and underestimated bond angles. The optimized geometries of the mAlH clusters are reported in Table 2, whereas their calculated shielding constants and chemical shifts are given in Table 3.

The downfield shift is maximum for the Al1 site, with a calculated ordering of $\delta_1 < \delta_8 < \delta_3$, which correlates with our assignment of Si sites based on the ^{29}Si chemical shifts. Since ^{27}Al is a quadrupolar nucleus, with spin 5/2, the NMR signals are broadened due to the large quadrupolar interaction, despite its 100% natural abundance.

The experimental ^{27}Al MAS NMR spectrum of zeolite Al-β shows a broad signal, 10 ppm wide, which can be deconvoluted into three bands.[14] The calculated ordering, using the group nomenclature, is thus $\delta_B < \delta_A < \delta_C$. As found previously for the Si sites, the more negative ^{27}Al chemical shift correlates with the larger $\langle$Al−O−Si$\rangle$ angle. Moreover, the decrease in $\langle$Al−O−Si$\rangle$ values going from Al1 to Al8 and to Al3 follows the same trend as the one found for the corresponding Si sites. Hence, our prediction that the −106.0 ppm signal corresponds to group B sites seems thus reasonable. For the two other bands, it may be argued from the comparison with the ^{29}Si spectrum that they could be due to groups of signals which are not straightforwardly classified as A and C. In fact, the assignment of the band with the least negative δ to some C sites, as is the case for ^{29}Si sites C3 and C4, is also suggested by the following arguments. In the experimental spectrum, the intensity of the band (δ_3 value here) decreases progressively when the zeolite is dealuminated, indicating a smaller stability for these Al sites. At the same time, the evaluation of the relative stabilities of aluminum in cluster models of sites B1, A8, and C3 shows that the latter corresponds indeed to the least stable Al site.[37] These results suggest that at least some of the sites C are related to the experimental band at −99.5 ppm.

As expected, the geometry optimization of these mAlH models leads to underestimated chemical shifts, with error of about 11 ppm with respect to the experimental values. This error is larger than for the corresponding mSi models, which can be related to a larger effect of the constraint (fixed border H atoms) on a necessarily more relaxed structure.

2. Two-Site Cluster Models. Since the cluster size is shown to be important for the description of absolute chemical shifts, we have then chosen to analyze the effect of increasing this size. Indeed, quantitative prediction of the chemical shifts for crystallographically distinct sites will increase the confidence in NMR techniques as a structure-determining tool.

The study of the mazzite zeolite showed that increasing the cluster size to an octamer $(H_3SiO)_3SiOSi(OSiH_3)_3$ leads to a substantial improvement of the NMR simulation. Mazzite is a highly symmetrical zeolite with only two crystallographically distinct Si sites, which can be included in the same octamer (2T) model. In the case of zeolite-β, the presence of all the next neighbor Si sites would imply a large cluster model containing nearly 17 Si sites, which is computationally demanding. Hence, we tried a fragment-averaging technique. The central silicon in a mSi cluster has four silicon neighbors. To build a double-site model (octamer), one of the four silicon neighbors of a mSi cluster is terminated by three $OSiH_3$ groups instead of three hydrogens, as shown in Figure 2 b−d. The same procedure is applied three more times to create three more octamers, wherein the other three silicon neighbors are saturated with $OSiH_3$ groups instead of hydrogens. This method has been used earlier to represent a pentamer cluster by four dimer clusters.[52]

The results of the calculations carried out on such octamer cluster models are given in Table 4, whereas their structures are illustrated in Figure 2b−d. To represent the influence of all the next neighbor silicons on the ^{29}Si NMR chemical shift of Si1, we considered four cluster models, namely, mSi1Si2, mSi1Si7, mSi1Si8, and mSi1Si3. The final chemical shift for site 1 is taken as an average of the four values. The ^{29}Si chemical shifts calculated by this procedure for Si1, Si3, and Si8 are given in Table 4. They are in excellent agreement with the experimental values, since these predicted chemical shifts are within an accuracy of 1 ppm. The same considerable improvement with respect to the 1T models was obtained for mazzite (2T model: $\delta_{calc} = -113.3$ and −103.4 ppm, compared to $\delta_{exp} = -113.1$ and −103.4 ppm).

We can also argue from these results that the calculated shielding constants are sensitive to the number of four-

(52) Vetrivel, R. *Zeolites* **1992**, *12*, 424.

Table 4. Comparison of Calculated and Experimental ^{29}Si Chemical Shifts, ppm, for the Different Si Sites in Polymorph A of Zeolite-β[a]

model	n_{4r}	Si1	Si2	Si3	Si4	Si5	Si6	Si7	Si8	Si9
mSi*n*		−113.0	−113.2	−106.6	−106.9	−109.4	−109.9	−111.0	−110.0	−108.8
mSi1Si2	1	−117.8	−117.9							
mSi1Si7	0	−115.0						−114.1		
mSi1Si8	0	−114.9							−112.9	
mSi1Si3	1	−117.2		−111.3						
mSi3Si4	2			−113.7	−114.0					
mSi3Si5	1			−110.5		−113.3				
mSi3Si8	0			−108.9					−112.2	
mSi8Si2	0		−115.3						−113.1	
mSi8Si6	0						−112.3		−112.8	
average		−116.2		−111.1					−112.8	
exp		−115.5	−116.0	−111.0	−111.6	−112.0	−113.0	−113.2	−111.8	−111.7

[a] n_{4r} is the number of four-membered rings attached to the Si site.

membered rings present in the model. Indeed, a given silicon site within models with the same number of four-membered rings has similar values of δ, whereas its chemical shifts differ for different numbers of four-membered rings (4.8 ppm for Si3 between the models mSi3Si8 (zero four-membered rings) and mSi3Si4 (two four-membered rings), for example). This shape effect suggests the opportunity to use a cluster with four coordination spheres (O, Si, O, Si) around the examined silicon atom, or equivalently to apply the described fragment-averaging technique, along with two sites, two-coordination-sphere cluster models, to reach quantitative results.

V. Conclusion

The ^{29}Si and ^{27}Al MAS NMR spectra of zeolite-β have been calculated, using the recently developed SOS-DFPT technique. The chemical shifts of the nine silicon sites have been first estimated using cluster models with a chemical formula of $Si(OSiH_3)_4$ and the geometry derived from the reported crystal structure.

From these models, each representing a single T site of the solid, we were able to assign the nine MAS NMR signals reported for a highly siliceous zeolite-β. These results reveal a linear correlation between the ^{29}Si NMR chemical shifts and the average Si−O−Si bond angles.

When the structures of these clusters were allowed to relax, fixing the border H atoms at the solid geometry, it was observed that the geometry relaxation causes a uniform downfield shift of about 5 ppm, due to the underestimation of the Si−O−Si angles in these small models.

However, the relative positions of the signals remain unchanged, allowing then a valid assignment of the spectrum.

The ^{27}Al NMR chemical shifts for the corresponding Al-containing cluster models have also been evaluated after relaxation of the cluster geometries, leading to a qualitative assignment of the wide band displayed by the experimental spectrum and deconvoluted into three signals.

Finally, larger cluster models with a chemical formula of $R_3SiOSiR_3$ ($R = OSiH_3$) have also been considered, representing double T sites in the zeolite lattice. We used a "fragment-averaging" technique to take into consideration the effects of next neighboring TO_4 units. The results obtained are extremely gratifying, reducing the error of the calculated chemical shifts to ± 1 ppm with respect to experimental values.

Thus, the present study has demonstrated a technique to calculate chemical shifts quantitatively. The MAS NMR technique combined with such quantum calculations could now be used as a "structure-determining" tool, particularly for the macroporous materials with smaller crystallite sizes (<5 μm), where the single-crystal structure determination is prohibitive.

These results indicate that the Si sites can be exactly assigned to distinct signals in the ^{29}Si NMR spectrum, using the SOS-DFPT method.

Acknowledgment. Financial assistance from IFCPAR (Project No. 1206-1) is gratefully acknowledged. Financial support from the Slovak Grant Agency Vega (Grant No. 2/3008/98) is gratefully acknowledged. Calculations were partially run on the NEC-SX4 of the CSCS (Manno, Switzerland).

Supporting Information Available: Table listing geometric parameters, numbering of atoms, and connectivity of the T−O−Si linkings for the T sites in zeolite-β (1 page, print/PDF). See any current masthead page for ordering information and Web access instructions.

JA980903G